MASTER CCPY KEEP FOR REPRODUCTION PURPOSES

REPORT DOCUMENTATION PAGE

Form Approved
OMB NO. 0704-0188

Public reporting burden for this collection of information is estimated to average 1 hour per response, including the time for reviewing instructions, searching existing data sources, gathering and maintaining the data needed, and completing and reviewing the collection of information. Send comment regarding this burden estimates or any other aspect of this collection of information, including suggestions for reducing this burden, to Washington Headquarters Services, Directorate for information Operations and Reports, 1215 Jefferson Davis Highway, Suite 1204, Arlington, VA 22202-4302, and to the Office of Management and Budget, Paperwork Reduction Project (0704-0188), Washington, DC 20503.

1. AGENCY USE ONLY *(Leave blank)*	2. REPORT DATE	3. REPORT TYPE AND DATES COVERED
	September 10, 1997	FINAL REPORT 4/1/94 - 7/31/97

4. TITLE AND SUBTITLE
Laser Interactions with Single Droplets

5. FUNDING NUMBERS
DAAH04-94-G-0031

6. AUTHOR(S)
Richard K. Chang

7. PERFORMING ORGANIZATION NAMES(S) AND ADDRESS(ES)
Richard K. Chang
Dept. of Applied Physics
Yale University
P.O. Box 208284
New Haven, CT 06520-8284

8. PERFORMING ORGANIZATION REPORT NUMBER

9. SPONSORING / MONITORING AGENCY NAME(S) AND ADDRESS(ES)
U.S. Army Research Office
P.O. Box 12211
Research Triangle Park,, NC 27709-2211

10. SPONSORING / MONITORING AGENCY REPORT NUMBER
ARO 32498.13-GS

11. SUPPLEMENTARY NOTES
The views, opinions and/or findings contained in this report are those of the author(s) and should not be construed as an official Department of the Army position, policy or decision, unless so designated by other documentation.

12a. DISTRIBUTION / AVAILABILITY STATEMENT
Approved for public release; distribution unlimited.

12 b. DISTRIBUTION CODE

19971204 146

13. ABSTRACT *(Maximum 200 words)*

Final report on past three and a quarter years of ARO support in two research areas: (1) nonlinear optical effects with single droplets, that act as high Q optical cavities; and (2) detection of bio- and nonbio-airborne particles. Research accomplishments in the first area consist of the following: a) laser induced surface bulge; b) mode beating among shape-distortion split resonance modes; c) temporal asymmetry of clockwise and counter-clockwise elastic scattering; d) model for optical bistability; e) external versus internal pumping of stimulated Raman scattering; f) second-harmonic generation from surfactant on hanging droplets, and g) application of chaos theory to optical cavities. Research accomplishments of the three joint ARL-Yale experiments in bio- and nonbio-airborne particle detection are summarized. In order to optimize data capture and storage, three schemes are discussed: (1) conditional sampling; (2) conditional firing; and (3) conditional storage.

DTIC QUALITY INSPECTED

14. SUBJECT TERMS	15. NUMBER IF PAGES
nonlinear optics, microcavities, biological particles, fluorescence spectra, elastic scattering, aerosols, microparticles, environmental detection	28
	16. PRICE CODE

17. SECURITY CLASSIFICATION OR REPORT	18. SECURITY CLASSIFICATION OF THIS PAGE	19. SECURITY CLASSIFICATION OF ABSTRACT	20. LIMITATION OF ABSTRACT
UNCLASSIFIED	UNCLASSIFIED	UNCLASSIFIED	UL

LASER INTERACTIONS WITH SINGLE DROPLETS

FINAL PROGRESS REPORT

RICHARD K. CHANG

AUGUST, 1997

U. S. ARMY RESEARCH OFFICE

ARO CONTRACT NO: DAAH04-94-G-0031
APRIL 1, 1994 - MAY 31, 1997

YALE UNIVERSITY
DEPARTMENT OF APPLIED PHYSICS AND CENTER FOR LASER DIAGNOSTICS
P. O. BOX 208284
NEW HAVEN, CONNECTICUT 06520-8284

APPROVED FOR PUBLIC RELEASE;
DISTRIBUTION UNLIMITED

THE VIEW, OPINIONS AND/OR FINDINGS CONTAINED IN THIS REPORT ARE THOSE OF THE AUTHOR AND SHOULD NOT BE CONSTRUED AS AN OFFICIAL DEPARTMENT OF THE ARMY POSITION, POLICY, OR DECISION, UNLESS SO DESIGNATED BY OTHER DOCUMENTATION.

CONTENTS

Figure Captions

Figure 1. Schematic for sampling only those fluorescence spectra that the PMT outputs have satisfied certain conditions in the logic unit. This scheme is only suitable for cw laser excitation, e.g., an argon ion laser emitting at 488 nm.

Figure 2. Schematic for firing a flashlamp Q-switched laser (266 nm) of low repetition rate. The laser is triggered only after the PMT outputs have satisfied certain conditions in the logic unit.

Figure 3. Schematic for storing only those fluorescence spectra that the PMT outputs have satisfied certain conditions in the logic unit. The storage rate of the ICCD detector is 10 Hz.

Figure 4. Experimental arrangements of the recent (April, 1997) joint ARL-Yale experiment. PMT 1 is to detect the elastic scattering. PMT 2 is to detect amino-acid fluorescence. PMT 3 is to detect the NADH fluorescence. PMT 4 is to detect the flavin fluorescence.

Figure 5. Chart that summarizes the laser, ICCD detector, and particle requirements. The pros and cons of the three experimental approaches are listed.

Figure 6. 100-shot averaged fluorescence spectra of single $(NH_4)_2SO_4$ with 266 nm and 355 nm excitation.

Figure 7. Same as Fig. 6, except for cigarette smoke.

Figure 8. Same as Fig. 6, except for Bacillus subtilis.

Figure 9. Same as Fig. 6, except for Escherichia coli.

Figure 10. Same as Fig. 6, except for Azotobacter Vinlandii.

Introduction

During the past three and a quarter years of ARO support, our research has been focused in two areas: (1) nonlinear optical effects with single droplets: and (2) detection of bio- and nonbio-airborne particles. The list of publications that resulted from our studies are found on page 11. At first glance, these two areas seem to be totally distinct. However, they share many experimental concerns in the generation of aerosols, collection of scattered radiation, isolation and dispersion of the wavelength-shifted scattering, and the detection of weak signals from micron-sized particles.

In the case of nonlinear optical effects with single droplets, we concentrate on the role the droplet as a micro-cavity in generating stimulated Raman scattering, stimulated Brillouin scattering, as well as lasing. In the case of detection of bio- and nonbio-airborne particles, we concentrate on detecting the elastic scattering by whole particles and the weak fluorescence from various biological molecules contained in the particle.

A brief summary of each of these two areas is presented. Much of the technical details on nonlinear optical effects with single droplets can be found in the technical reports and reprints of publication, that have been sent to ARO. In the bio-airborne particle detection area, the most recent ARL-Yale joint experiment was conducted at Yale in April, 1997. The data is being analyzed and the details of the experiments are being written up for publication in a special issue on bio-detection and sensors, to be published in Aerosol Science and Technology. Consequently, in this report a bit more detail is provided on the latest ARL-Yale joint experiment.

Research Accomplishments

I. Nonlinear optical effects with single droplets

The curved liquid-air interface of droplets gives rise to quasi-total internal reflection for the incident and internally generated waves. Because of the curved liquid-air interface, some of the internal radiation can leak out of the droplet even though in the geometric optics model, the rays are incident with an angle larger than the critical angle for total internal reflection. Thus a droplet can be treated as a micro-cavity with a slight amount of leakage, i.e., micro-cavity with high Q-factor values. The cavity modes of such a dielectric particle and their effects in enhancing the nonlinear optical processes are summarized in two "review-type" papers (see Publications A and B). The potential application of such nonlinear optical spectroscopy to the diagnostics of fuel sprays has been summarized in another review-type paper (see Publication C).

Some of the new observations and explanation of nonlinear optical effects with single droplets are briefly summarized below.

a) Laser-induced bulge that enhances input coupling

Thus far, most of the experimentalists use a single high-intensity laser pulse to generate the nonlinear optical effects. A surprising observation was made when a train of high-intensity pulses (each 100 psec long and separated by 13.2 nsec) irradiates a single droplet. The droplet behaves as if it "remembers" the occurrence of the previous series of pulses. After ruling out the retention of photons by the droplet cavity, we proposed a model that invokes the laser-induced effect.

When a 100 sec pulse is impinged on the edge of a droplet, the internal field of the laser is imhomogenuous. The highly localized illumination area, just within the shadow face and the equator, imparts an impulse to the droplet and causes the droplet surface to bulge. The bulge continues to grow in between the laser pulses (separated

by 13.2 nsec). Initially, when the bulge amplitude is small and the curvature is large, more of the pump laser light can be coupled into the droplet, and more of the nonlinearly generated light can be coupled out of the droplet.

The experimental results with a different number of pulses indicated that for a given pulse intensity, there is an optimum number of pulses that can create a highly localized bulge that improves the input coupling without degrading the overall Q so significantly that the round-trip loss (due to leakage) exceeds the pump-intensity dependent round-trip gain.

Our publication (see Publication D) will appear in JOSA B this November.

b) Mode beating of shape-distortion split resonance modes

For a perfectly spherical droplet, the azimuthal modes (designated by m's) are $2n + 1$ degenerate, where n is the mode number or the effective angular momentum of the microcavity modes. The n is equal to the one half the number of wavelengths that can fit inside the droplet circumference.

For slightly deformed droplets (a quadrupolar deformation, in the shape of oblate or prolate spheroid), the m-modes are split, where each of the doubly degenerate m-modes has a unique frequency. The double degeneracy remains because the sense of rotation (clockwise or counterclockwise) is not destroyed by shape deformation.

In the past, we have observed the frequency splitting m-modes in the frequency domain with a Fabry-Perot interferometer and a spectrograph.

Depending on the frequency splitting and the cavity-lifetime of the m-modes, an experimentalist may find it more convenient to measure the mode separation in the frequency or time domain. The previous observation of precession of the m-modes (detected in the time domain) is also a manifestation that the m-modes are frequency split because of shape deformation. Recently, we have observed the temporal beating between the m-modes that are localized around the droplet equator. By collecting the

nonlinearly generated stimulated Raman scattering from only a small area at the equator, only a few *m*-modes are involved and they are equally separated in frequency (to first order of the deformation amplitude). Thus, the difference frequency between neighboring *m*-modes are nearly equal. The detected signal contains an oscillatory part, with the fundamental oscillation frequency equal to the frequency difference of the *m*-modes. More details are provided in Publication E.

c) Temporal asymmetry of the forward- and backward-elastic scattering

We have investigated spatially resolved scattering of green light (at 532 nm) from various parts of the droplet, when a train of picosecond pulses (at 532 nm, 100 psec pulse duration, and 13.2 nsec pulse-to-pulse separation) of a focused laser beam is incident on part of a droplet surface.

The forward-circulating light from the ethanol droplet exhibits a smooth, delayed pulse-to-pulse nonlinear growth attributed to increased input coupling into Q-degraded MDR. The mechanism for Q-degradation is laser-induced electrostriction at the laser focal spot, causing a surface bulge of small amplitude and large curvature, exactly like the surface bulge mentioned previously in Section a on page 2. The forward-circulating light is just a manifestation of the enhanced input coupling of the external laser beam into the cavity modes of the droplet.

In contrast, the backward-circulating might, from the ethanol droplet, exhibit an irregular pulse-to-pulse nonlinear growth attributed to near-backward stimulated Brillouin (SBS) resonant on a high-Q cavity mode. We did not completely confirm that the backward-circulating signal was indeed the SBS, because no attempts were made to measure the frequency difference between the forward- and backward-circulating signals. For details see Publication F.

The results of Sections a, b, and c are summarized in "review" type chapter of a CRC publication (for details see Publication G).

d) Model for optical bistability

We have investigated the role of a sphere with an intensity-dependent refractive index $m(\mathbf{r}) = m_0 + m_2 I(\mathbf{r})$, where $I(\mathbf{r})$ is the internal intensity at position $\mathbf{r}$. When the incident frequency is a few linewidths away from a resonance mode of microparticle cavity, optical bistability effects are expected. A discussion is made (in Publications H and I) on the similarities and the differences between optical bistability in a conventional Fabry-Perot cavity and a spherical cavity. Numerical estimates were made on the input intensity need for a CS_2 sphere to exhibit optical bistability when the input laser frequency is 10 to 40 linewidths from a sphere's resonant mode with Q $= 5.5 \times 10^5$.

e) External versus internal pumping of stimulated Raman scattering (SRS).

The SRS signal from weaker gain vibrational modes or from the minority species in a binary mixture droplet is small, because of depletion of the pump beam by the strongest-gain vibrational Raman mode. The Raman gain for a given vibrational mode is dependent on which cavity-resonance mode is providing the optical feedback at the Raman-shifted frequency, as well as the spatial overlap between that cavity-resonance mode and the pump radiation. The spatial overlap can be very good between the SRS of the major species and the cavity-resonance mode of the SRS of the minor species. Whereas, the spatial overlap is poor between the internal fields of the input-pump laser (off an input cavity resonance) and the cavity-resonance mode of the SRS of the minor species. The spatial distribution of the SRS of the major species is similar to that of the cavity resonance mode which provides the feedback for the SRS of the minor species. The contrary is true for the spatial distribution of the internal distribution of the input-pump radiation (if that is off an input cavity

resonance), as it is localized in a small regime with little overlap with the spatial distribution of the cavity resonances.

To generalize our experimental results, we present an effective-average Raman gain formula and discussed the various factors that contribute to the enhancement of the SRS relative to input-pumping approach. In addition, we summarized all the different experimental schemes whereby the SRS, from a minor species, can be enhanced. These schemes include the following: (1) fluorescence seeding by adding a dye into the solution to provide some extra radiation in the spontaneous Raman wavelength range; (2) resonance Raman enhancement by selecting the input-laser wavelength in the absorption band of the minor species and in the transparent band of the major species; and (3) external seeding by introducing some extra radiation (at the wavelength of the spontaneous Raman wavelength range) before the onset of the input-pump radiation. For details see Publication J.

f) Second-harmonic generation (SHG) from surfactants on hanging droplets

In the electric dipole approximation, SHG from isotropic medium (with center of inversion) is forbidden. However, from aligned molecules located on the liquid-air interface and oriented perpendicularly to this interface, SHG is allowed in the electric dipole limit. SHG, from surfactant on a flat liquid-air interface, has been seen by several active groups for at least two decades.

We were interested in observing the SHG from surfactant sub layer on micrometer-sized droplets. Because we were using flowing droplets, the time that the droplets traverse 5 cm downstream from the Burglund-Liu droplet generator exit aperture is too short for all the large surfactant molecules to diffuse from the droplet interior to the droplet surface. We had to use a "stationary" droplet, that hangs on the end of a tapered optical fiber.

SHG was indeed observed from a pendent-shape droplet hanging on the tip of a tapered fiber. From the polarization dependence of the SHG that was confirmed by the polarization dependence of the fluorescence from the same surfactant layer, we were able to deduce that the surfactant orientation were NOT laying on the liquid-air interface, but is slightly tilted toward the normal to the interface. We did not have time to finish the study of role of the nearly circular interface on surface SHG. For details is Publication K.

g) The application of chaos theory to optical microcavities.

Our experimental efforts in spherical and nearly spherical droplets have piqued the interest of one theoretical colleague, A. Douglas Stone, in the Department of Applied Physics, to apply the tools of chaos theory to ray dynamics within a deformed microcavities. The ray dynamics applied is a three-dimensional "billiard", that specular reflects from the liquid-air interface, with the condition that if the incident angle falls below the critical angle then the ray escapes according to Snell's law. The lowering of the Q factor of the resonant mode associated with a deformed sphere can be understood as a transition to chaotic ray dynamics which can no longer be confined by total internal reflection. For more details see Publication L.

For a special class of deformed spheres, for example, objects that possess axisymmetry, it is possible to use chaos ray dynamics to predict theoretically several properties of the resonant cavity modes, e.g., the Q of the resonant modes; the locations on the curved interface where the most of the light will leak; and the angular distribution of the leaking rays external of the cavities. The chaos ray dynamics approach is not compute intensive and provide an intuitive picture of what is occurring with rays trapped within the asymmetric object. For more details see Publication M.

II. Detection of bio- and nonbio-airborne particles

The distinction between bio- and nonbio-airborne particles is totally dependent on the assumption that biological airborne particles **must** contain some amino acid (fluorescent at 350 nm) and may contain some NADH (fluorescent at 450 nm), and flavins (fluorescent at 550 nm). We further assume that nonbio particles do not have fluorescence at the amino acid fluorescent wavelength region. The airborne particles are channeled through a tube to a nozzle, exit from the nozzle, and then flow into the laser focal volume. Because the arrival of particle at the laser focal volume is statistical, several strategies have been employed to maximize the chances of having a flowing particle in the focal volume each time the laser fires and to store the entire fluorescent spectra only from those particles that have fluorescent emission in the amino acid band (around 350 nm). Different strategies are used for various laser-detector combinations, depending whether the laser is cw or pulsed, whether the repetition rate of the pulsed laser is low or high, and whether the particle density is sparse or abundant.

Two years ago (April, 1995) when we were conducting our first joint experiment (with Drs. Steve Hill and Ronald Pinnick at White Sands Missile Range), we used a cw argon laser (514.5 nm) and the intensified-charge coupled detector (ICCD) that was conditionally gated-on, whenever a photomultiplier (PMT) detected the elastic scattering (or fluorescence within a given wavelength band) from a flowing particle just upstream from the laser focal volume (see Fig. 1). We designated this technique as "**Conditional Sampling**", because the ICCD detector was gated-on and sampled the entire fluorescence spectrum only if specific conditions were fulfilled with the PMT outputs.

In December 1996, when we were conducting our second joint experiment, we used a pulsed UV laser (266 nm) and ICCD detector. Because both the UV pulsed laser and the ICCD detector have low repetition rates (10 Hz), we had to make sure we fire the laser only when there was a particle (at upstream) that will subsequently flow into the laser focal volume. Figure 2 shows that a cw laser (488 nm from an argon laser) was focused a

few millimeters above the focal volume of the pulsed UV laser. The flowing particle stream is assumed to have a straight trajectory in the downward direction. The two PMT's detected the elastic scattering and/or the fluorescence. The PMT outputs were fed into a logic unit and its output (with a time delayed that is commensurate with the particle time-of-flight) triggered that pulsed UV laser and gated on the ICCD detector. We named this approach as "**Conditional Firing**", because the laser is fired, conditioned on the PMT outputs, which when fed to the logic unit would only produce a trigger signal if certain conditions were satisfied.

In April 1997, when we were conducting our third joint experiment, we used a high repetition rate pulsed UV laser (266 nm, at 2 kHz) and the same ICCD detector (at 10 Hz). Because the ICCD detector is the "slowest" element, we only wanted to store the ICCD detector data whenever the PMT outputs satisfy certain logic conditions (see Fig. 3). Hence we named this technique "**Conditional Storing**".

The PMT arrangements fused in our April 1997 joint ARL-Yale experiment are shown in Fig. 4. In specific, PMT 1 is for detecting the elastic scattering, PMT 2 is for amino acid detection, PMT 3 is for NADH detection, and PMT 4 is for flavin detection. The chart in Fig. 5 summarizes the three conditionally triggering schemes, in term of how the lasers and ICCD detector are operating (external triggered versus free running), particle density loading necessity for straight trajectory, and finally the pro and con of each scheme.

Figure 6 shows the 100-shot average of $(NH_4)_2SO_4$ particles when illuminated by the 266 nm laser and the 355 nm. $(NH_4)_2SO_4$ particles were chosen as our "null" sample because $(NH_4)_2SO_4$ exist naturally in the environment. For the 266 nm excited fluorescence spectrum, the 266 nm peak is just elastic scattering that is leaking through the long-pass fluorescence filters. The 532 nm peak is simply elastic scattering of the pump radiation (at 532 nm) leaking through the fluorescence filters. Recall that the 266 nm radiation is generated by a BBO second-harmonic crystal with the 532 nm as the pump. For the 355 nm excited spectrum, (see Fig. 6) the 532 nm peak is again the elastic

scattering of the pump leaking through the long-pass fluorescence filters. Note that the 355 nm radiation is generated by another BBO sum-frequency crystal, with the 532 nm and 1064 nm as the two input pumps. Both the 266 nm and the 355 nm excited spectra for do not exhibit any detectable fluorescence at the amino acid and NADH bands.

Figure 7 shows the 266 nm excited fluorescence spectrum (with 100 laser shot averaged) of cigarette smoke. Similarly, the two peaks at 266 nm and 532 nm are both associated with elastic scattering at these two wavelengths. With 266 nm excitation the small peak centered at 350 nm is associated with amino acid (trytophan). No detectable peak at the NADH fluorescence wavelength region was found. However, with 355 nm excitation, the fluorescence wavelength characteristic of NADH is clearly observable.

Figure 8 shows the 266 nm and 355 nm excited fluorescence spectra of bacillus subtilis. The amino acid trytophan fluorescence peak at 350 nm is the only peak observed with 266 nm excitation and the NADH fluorescence peak at 450 nm is the only peak observed with 355 nm excitation. Similar observations were made of the fluorescence spectra of escherichia coli and azotobacter vinlandii. In fact for most biological particles we only observe the tryptophan fluorescence peak at 350 nm when excited by 266 nm and observe the NADH fluorescence peak at 450 nm when excited by 355 nm.

Single particle fluorescence spectra were still noisy with low signal-to-noise ratio. In the future we intend to optimize the laser pulse intensity, pulsewidth, the collection optics, spectrograph, and ICCD detection system in order to, improve the signal-to-noise ratio of single particle fluorescence spectrum.

List of Publications that Acknowledged ARO DAAH04-94-G-0031

A. Richard K. Chang, Gang Chen and Md. Mohiuddin Mazumder, "Nonlinear Optics in Micro-Meter Sized Droplets," in Proceedings of the NATO ASI Series E, 314, 75 - 99, edited by M. Ducloy and D. Bloch (Les Houches France, 1995), Kluwer Academic Publishers, The Netherlands, 1996.

B. Gang Chen, Md. Mohiuddin Mazumder, J. Christian Swindal, Karl Schaschek, and Richard K. Chang, "Nonlinear Optical Emission and Scattering in Micrometer-sized Droplets," in Proceedings of the AGARD Symposium on High Power Microwaves (HPM), Ottawa, Canada, May 2-5, 1994, AGARD CP-564 (NATO, Neuilly Sur Sein, France 1995, p. 24-1.

C. Gang Chen, Md. Mohiuddin Mazumder, Richard K. Chang, J. Christian Swindal and William P. Acker, "Laser Diagnostics for Droplet Characterization," Progress in Energy & Combustion Science 22, 163 (1996).

D. Jürgen Popp, Mitchell H. Fields, Richard K. Chang, "Injection Seeding of Lasing in Microdroplets," Opt. Lett. 22, 139 (1997).

E. Jürgen Popp, Mitchell H. Fields, and Richard K. Chang, "Q-Switching by Saturable Absorption in Mircodroplets: Elastic Scattering and Laser Emission," Opt. Lett.22, 1296 (1997).

F. Janice L. Cheung, Justin M. Hartings and Richard K. Chang, "Different Temporal Behavior for the Forward- and Backward-Circulating Radiation within a Microdroplet," Opt. Lett. 20 1089 (1995).

G. J. L. Cheung, J. M. Hartings, and R. K. Chang, "Nonlinear Optics of Microdroplets Illuminated by Picosecond Laser Pulses," in Handbook of Optical Properties, Vol.II, *Optics of Small Particles, Interfaces and Surfaces* , CRC Press, p.223 (1996).

H. Md. Mohiuddin Mazumder, Steven C. Hill, Dipakbin Q. Chowdhury, and Richard K. Chang, "Dispersive Optical Bistability in a Dielectric Sphere," J. Opt. Soc. Am. B 12, 297 (1995).

I. Md. Mohiuddin Mazumder, Dipakbin Q. Chowdhury, Steven C. Hill, and Richard K. Chang, "Optical Resonances of a Spherical Dielectric Microcavity: Effects of Perturbations," in Optical Processes in Microcavities, edited by Richard K. Chang and Anthony J. Campillo, (World Scientific Publishers), p 209 (1996).

J. Md. Mohiuddin Mazumder, Mitchell H. Fields, Justin M. Hartings, Xiaoyun Pu, Alfred S. Kwok, Karl Schaschek and Richard K. Chang, "Enhancing Stimulated Raman Scattering of Weaker Gain Raman Modes in Microdroplets by Seeding and Efficient Pumping," in Nonlinear Frequency Generation and Conversion, Vol. 27 (SPIE, Bellingham, Washington, 1996) P. 352.

K. Justin Hartings, Xiaoyun Pu, Janice L. Cheung, Richard K. Chang, "Laser induced distortion for increased input coupling of light to droplet-cavity modes," JOSA B (to be published).

Publications, Cont.

L. A. Mekis, J. U. Nöckel, G. Chen, A. D. Stone and R. K. Chang, "Chaos and *Q*-spoiling in Lasing Droplets, " Phys. Rev. Lett., 75, 2682 (1995).

M. Jens U. Nöckel, A. Douglas Stone, Gang Chen, Helen L. Grossman and Richard K. Chang, "Directional Emission from Asymmetric Resonant Cavities," Opt. Lett. 21, 1609 (1996).

Invited Talks

"Nonlinear Optical Emission and Scattering in Micrometer-Sized Droplets," AGARD Symposium on High Power Microwaves (HPM), Ottawa, Canada, May 4, 1994.

"Nonlinear Optics in Micro-Meter Size Droplets, NATO Advanced Study Institute Conference on Quantum Optics of Confined Systems, Les Houches, France, May 23 - June 2, 1995 (two lectures).

"Optical Diagnostics of Droplets," Gordon Conference, Plymouth, New Hampshire, October 10, 1995.

"Nonlinear Spectroscopy of Species within Microcavities," Americal Chemical Society, San Francisco, April 13 - 17, 1997.

"Nonlinear Spectroscopy with Microspheres: Mechanisms and Applications," 13th International Conference on Laser Spectroscopy, Hangzhou, China, June 3-7, 1997.

Lectures

"Determination of Flowing Droplet Properties from Stimulated Light Emission: Chemical Engineering Department, University of Maryland, College Park, MD, September 13, 1994.

"What can we learn about the Physical and Chemical Properties of Droplets from Nonlinear Spectroscopy?" Physics Department, Worcester Polytechnic Institute, Worcester, MA, November 7, 1994.

"Nonlinear Spectroscopy of Multicomponent Droplets" Physics Department, New Mexico State University, Las Cruces, NM, November 16, 1994.

"Lasing Spectral Shifts Caused by Perturbations in Microdroplets", ICONO/LO '95 Conference, St. Petersburg, Russia, June 26, 1995.

"Physics and Applications of Microcavities" Corning, Inc., Corning, NY, Oct. 20, 1995.

"Optical Diagnostics of Droplets: Temperature and Physical and Chemical Properties" Caltech, Pasadena, CA May 19, 1996.

"Nonlinear Optical Interactions in Microdroplets; Possible Appications?" Northwestern University, May 16, 1996.

"Nonlinear Spectroscopy of Multicomponent Droplets", AFOSR Contractors Meeting, Virginia Beach, June 3-7, 1996.

"Optics within a Micrometer-Sized Cavity: An Overview," Dept. of Physics, Universite Claude Bernard, Lyon, March 13, 1997.

"Stimulated-Raman Scattering in Micro Droplets," Physics Dept., Fudan University Shanghai, PRC, June 9, 1997.

Students Awarded with Ph.D.

J. Christian Swindal, Ph.D., "In-Situ Characterization Techniques for Droplets and Sprays Using Nonlinear Optics," May 1994

Janice L. Cheung, Ph.D., "Interaction of a Train of Picosecond Laser Pulses with Microdroplets," May 1995

Md. Mohiuddin, Ph.D., "Perturbation Effects on Microsphere Resonances: Device Applications and Diagnostics," May 1996

Justin M. Hartings, Ph.D., "Characterization of Microdroplets with Mode-Locked Laser Pulses," May 1997

Scientific Collaborators

William Acker, Texaco Research, Beacon, New York

Gang Chen, Corning Research, Corning, New York
(was a Post-Doctoral Research Associate at Yale University)

Janice L. Cheung, Post-Doctoral Research Associate, Worcester Polytechnic Insitute
(was a graduate student at Yale University)

Dipakbin Q. Chowdhury, Corning Research, Corning, New York
(was a Post-Doctorial Research Associate at Yale University)

Mitchell H. Fields, Research Staff, Lincoln Lab., Lincoln, Massachusetts
(was a graduate student at Yale University)

Justin M. Hartings, Capt. in the U. S. Army (was a graduate student at Yale University)

Steve C. Hill, Army Research Laboratory, Adelphi, Maryland

Alfred S. Kwok, Assistant Professor, Franklin and Marshall College, Lancaster, Pennsylvania (was a graduate student at Yale University).

Md. Mohiuddin Mazumder, Intel, Santa Clara, California
(was a graduate student at Yale University)

Ronald G. Pinnick, Army Research Laboratory, Adelphi, Maryland

Xiaoyun Pu, Associate Professor, Yunnan University, Kunming, China
(was a Post-Doctoral Research Associate at Yale University)

Karl Schaschek, Reasearch Associate, Würzberg University, Würzberg, Germany
(was a Post-Doctoral Research Associate at Yale University)

A. Douglas Stone, Professor, Yale University, New Haven, Connecticut

Report of Inventions

None

Conditional Sampling

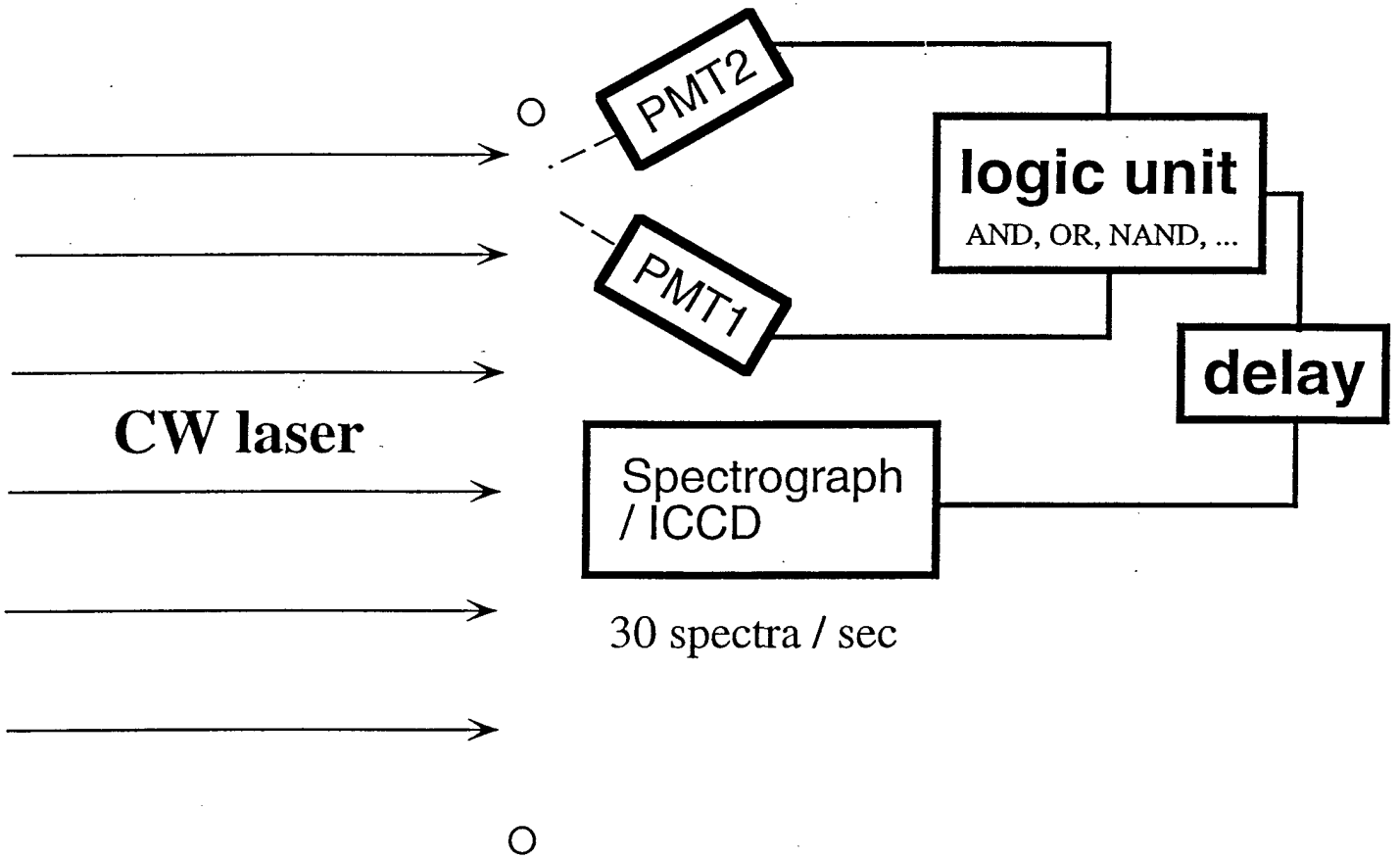

FIGURE 1. Schematic for sampling only those fluorescence spectra that the PMT outputs have satisfied certain conditions in the logic unit. This scheme is only suitable for cw laser excitation, e.g., an argon ion laser emitting at 488 nm.

Conditional Firing

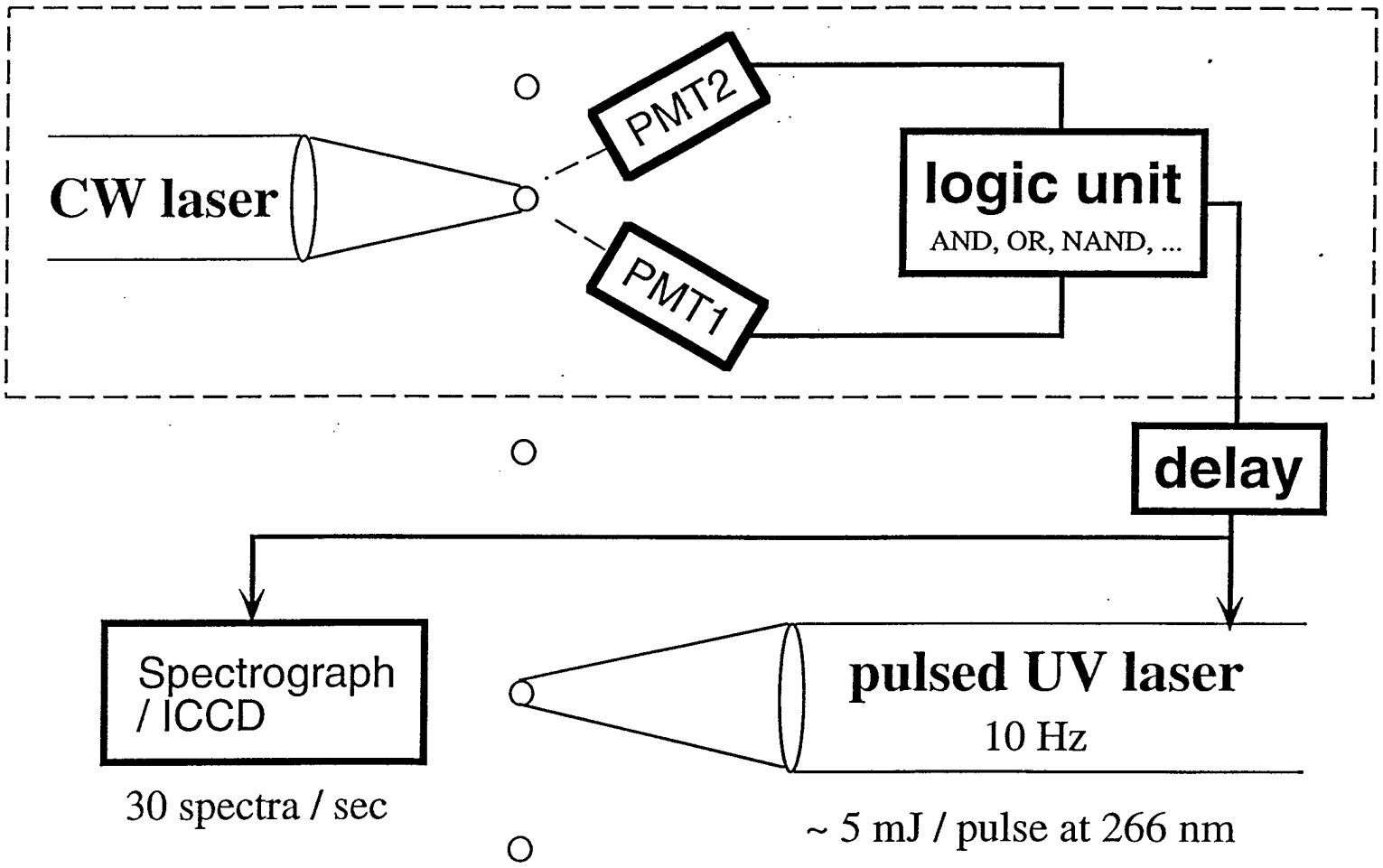

FIGURE 2. Schematic for firing a flashlamp Q-switched laser (266 nm) of low repetition rate. The laser is triggered only after the PMT outputs have satisfied certain conditions in the logic unit.

Conditional Storing

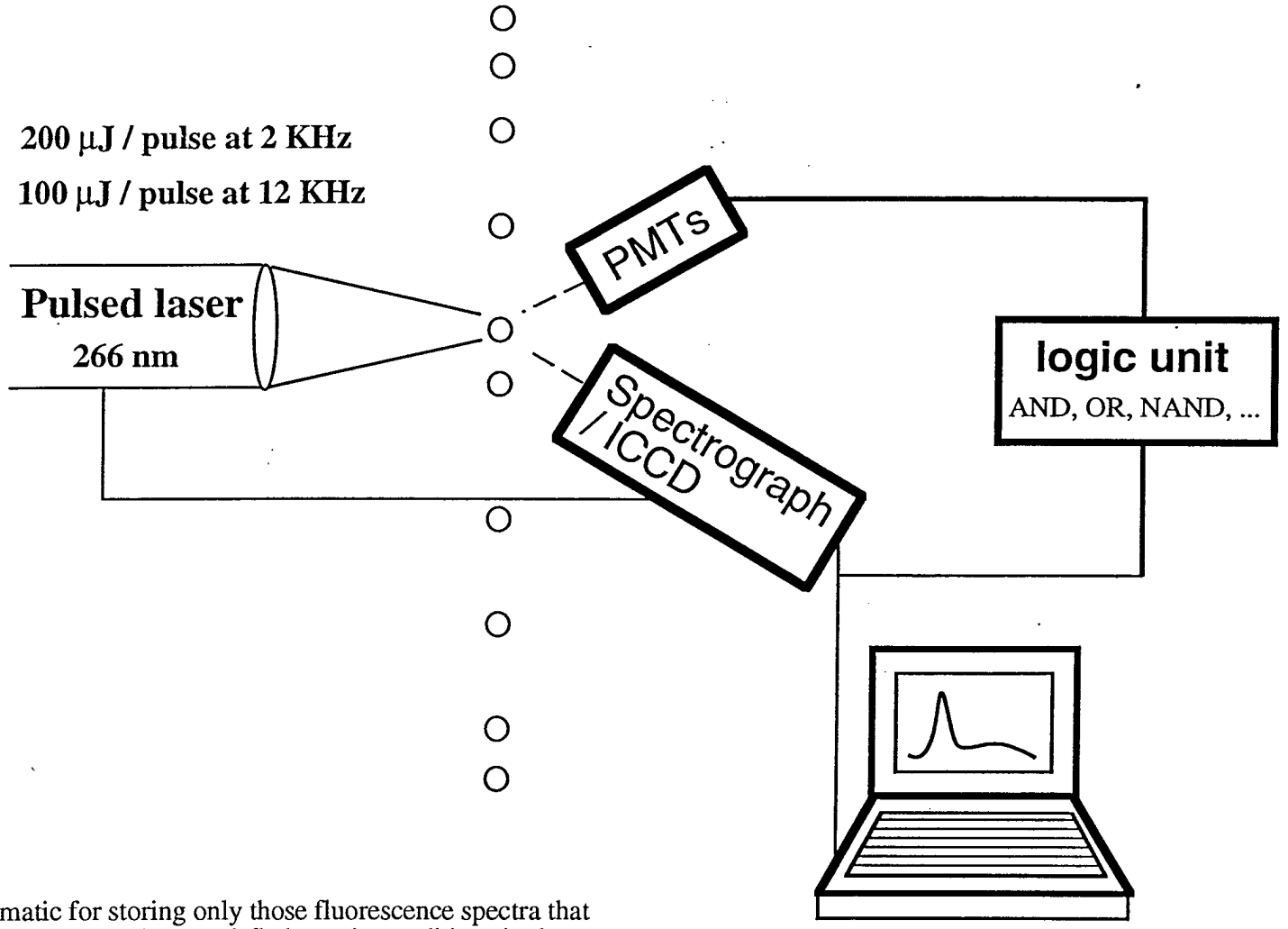

FIGURE 3. Schematic for storing only those fluorescence spectra that the PMT outputs have satisfied certain conditions in the logic unit. The storage rate of the ICCD detector is 10 Hz.

Fluorescence Spectral Analyzer and Multiwavelength Counter

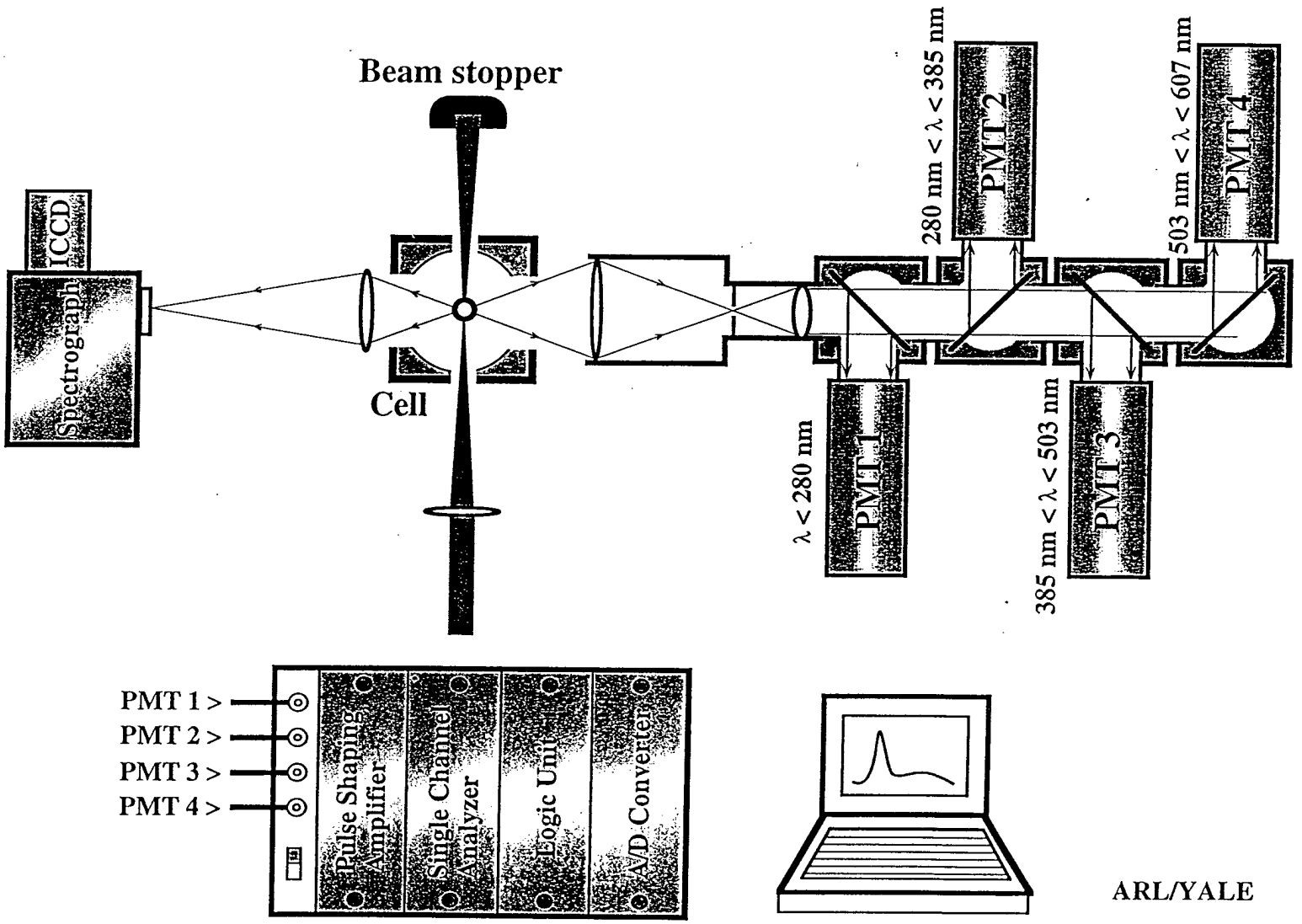

FIGURE 4. Experimental arrangements of the recent (April, 1997) joint ARL-Yale experiment. PMT 1 is to detect the elastic scattering. PMT 2 is to detect amino-acid fluorescence. PMT 3 is to detect the NADH fluorescence. PMT 4 is to detect the flavin fluorescence.

Conditionally	**Lasers**	**CCD**	**Particles**	**Pro**	**Con**
Sampling	cw	triggered by PMT	low density straight trajectory	1 laser	UV cw ? straight flow
Firing	cw pulsed (triggered)	triggered by PMT	low density straight trajectory	large signal	2 lasers straight flow
Storing	pulsed (free run)	free running, but stored by PMT	high density	1 laser any flow	missing or multiple particles ?

FIGURE 5. Chart that summarizes the laser, ICCD detector, and particle requirements. The pros and cons of the three experimental approaches are listed.

100-shot average of spectra of single aerosol particles (conditional storing)

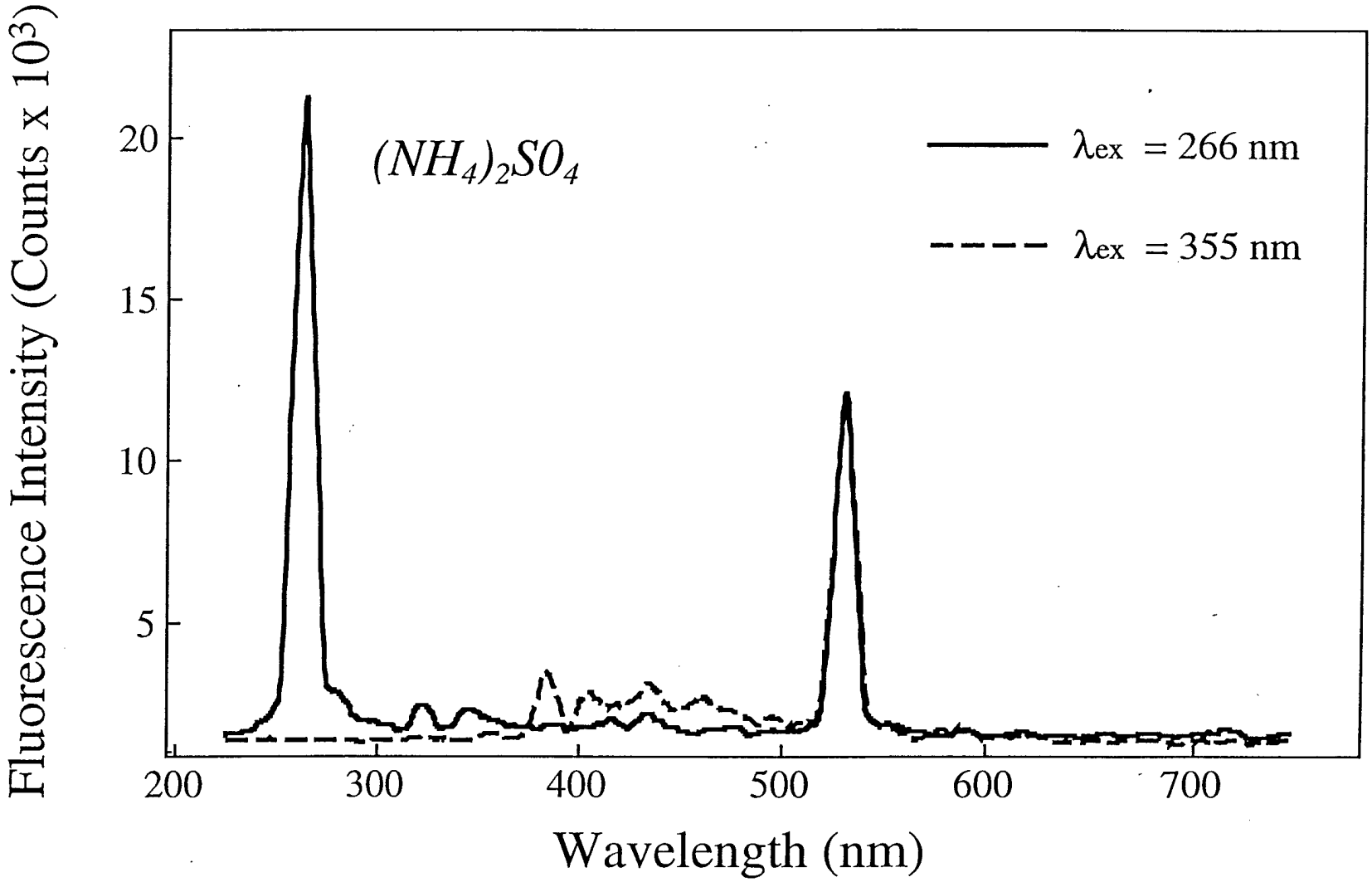

FIGURE 6. 100-shot averaged fluorescence spectra of single $(NH_4)_2SO_4$ with 266 nm and 355 nm excitation.

100-shot average of spectra of single aerosol particles (conditional storing)

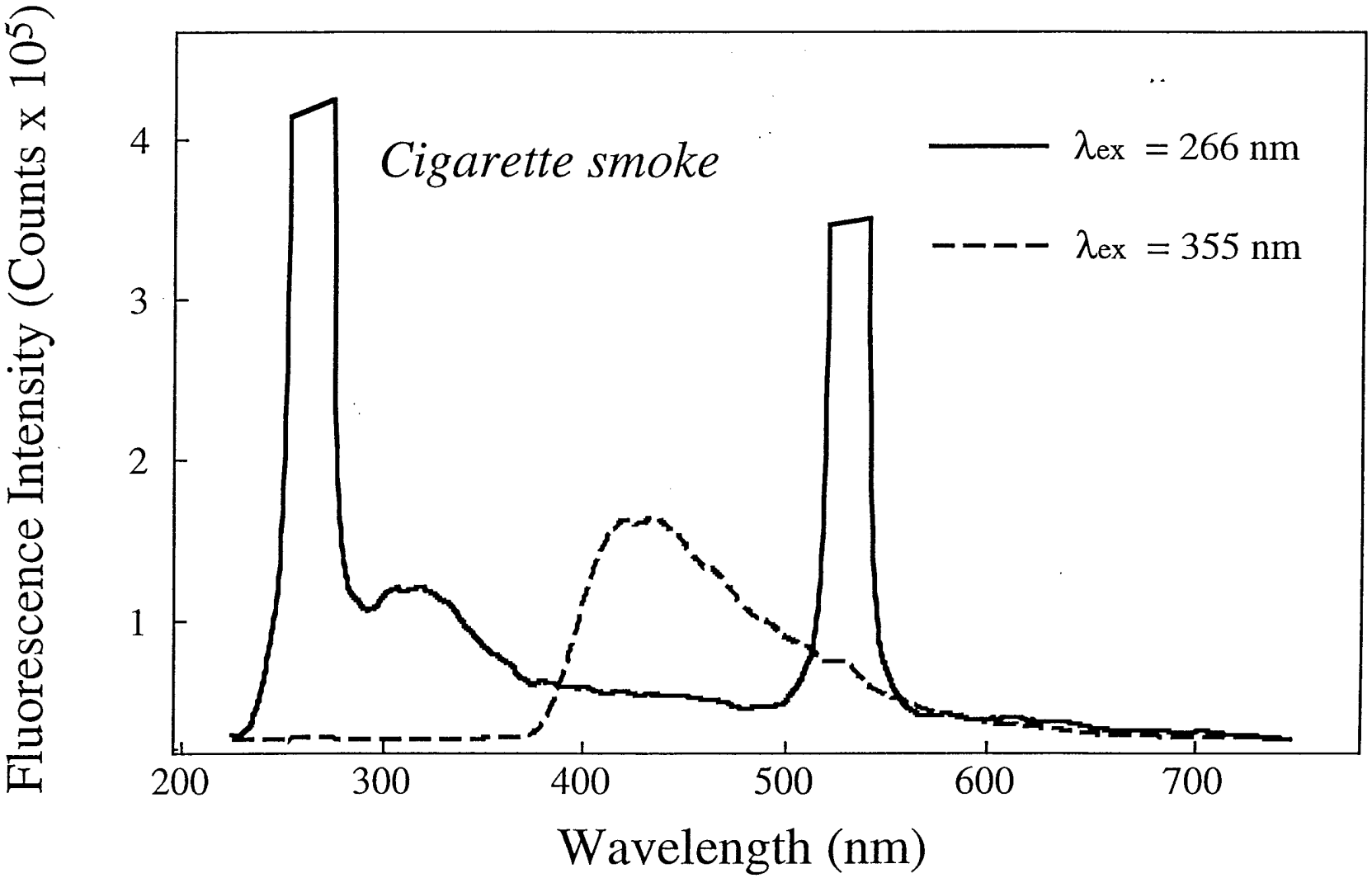

FIGURE 7. Same as Fig. 6, except for cigarette smoke.

100-shot average of spectra of single aerosol particles (conditional storing)

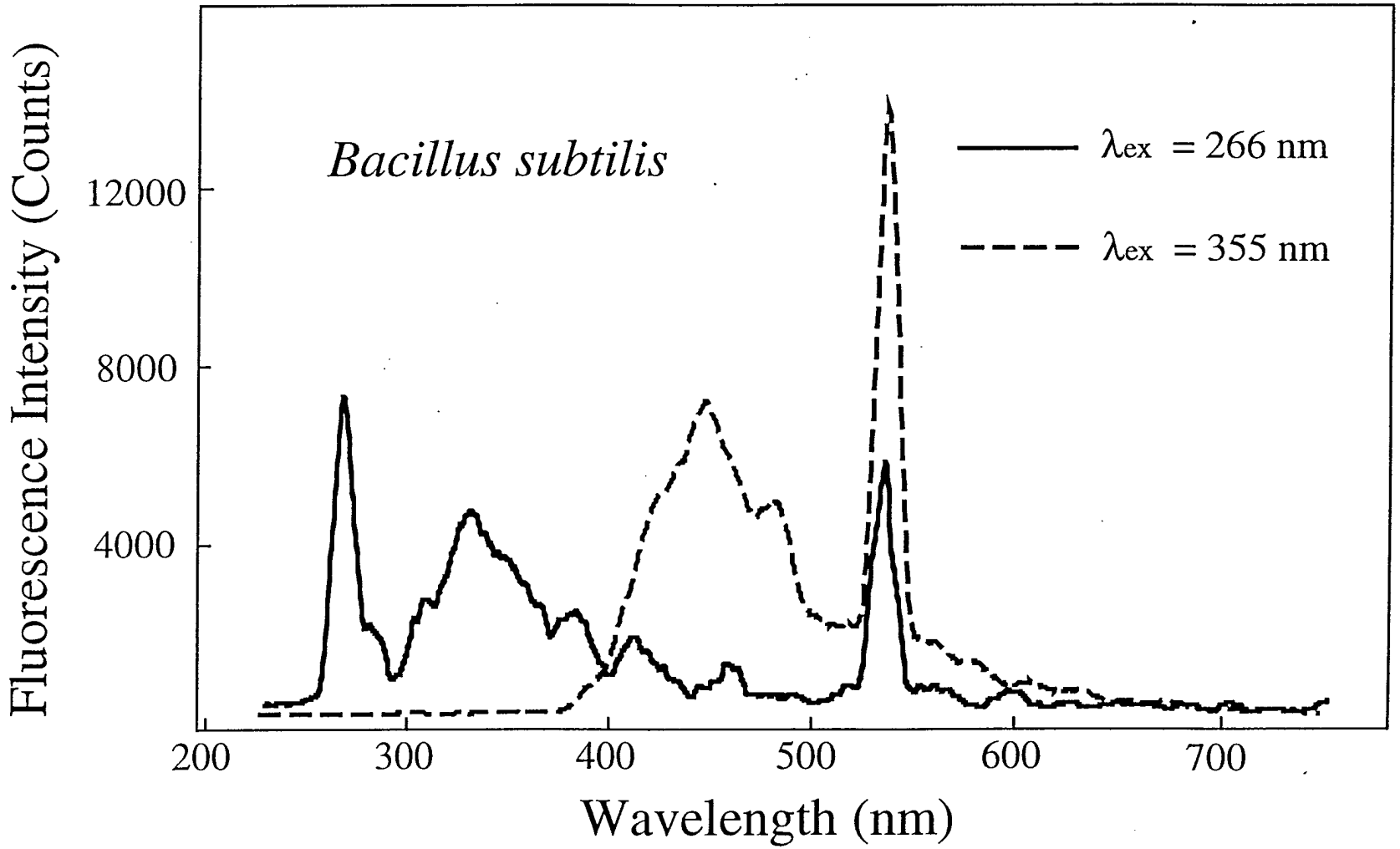

FIGURE 8. Same as Fig. 6, except for Bacillus subtilis.

100-shot average of spectra of single aerosol particles (conditional storing)

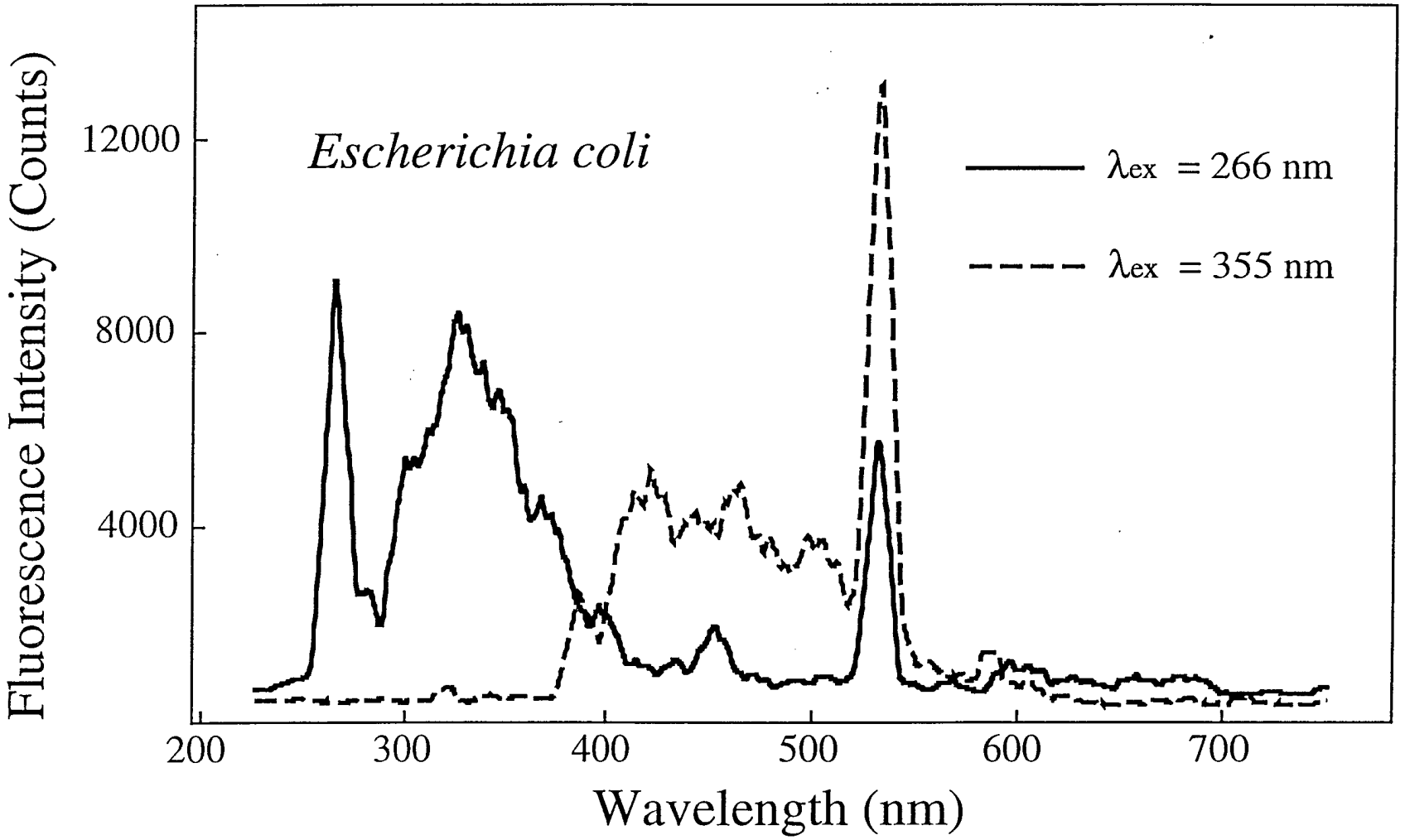

FIGURE 9. Same as Fig. 6, except for Escherichia coli.

100-shot average of spectra of single aerosol particles (conditional storing)

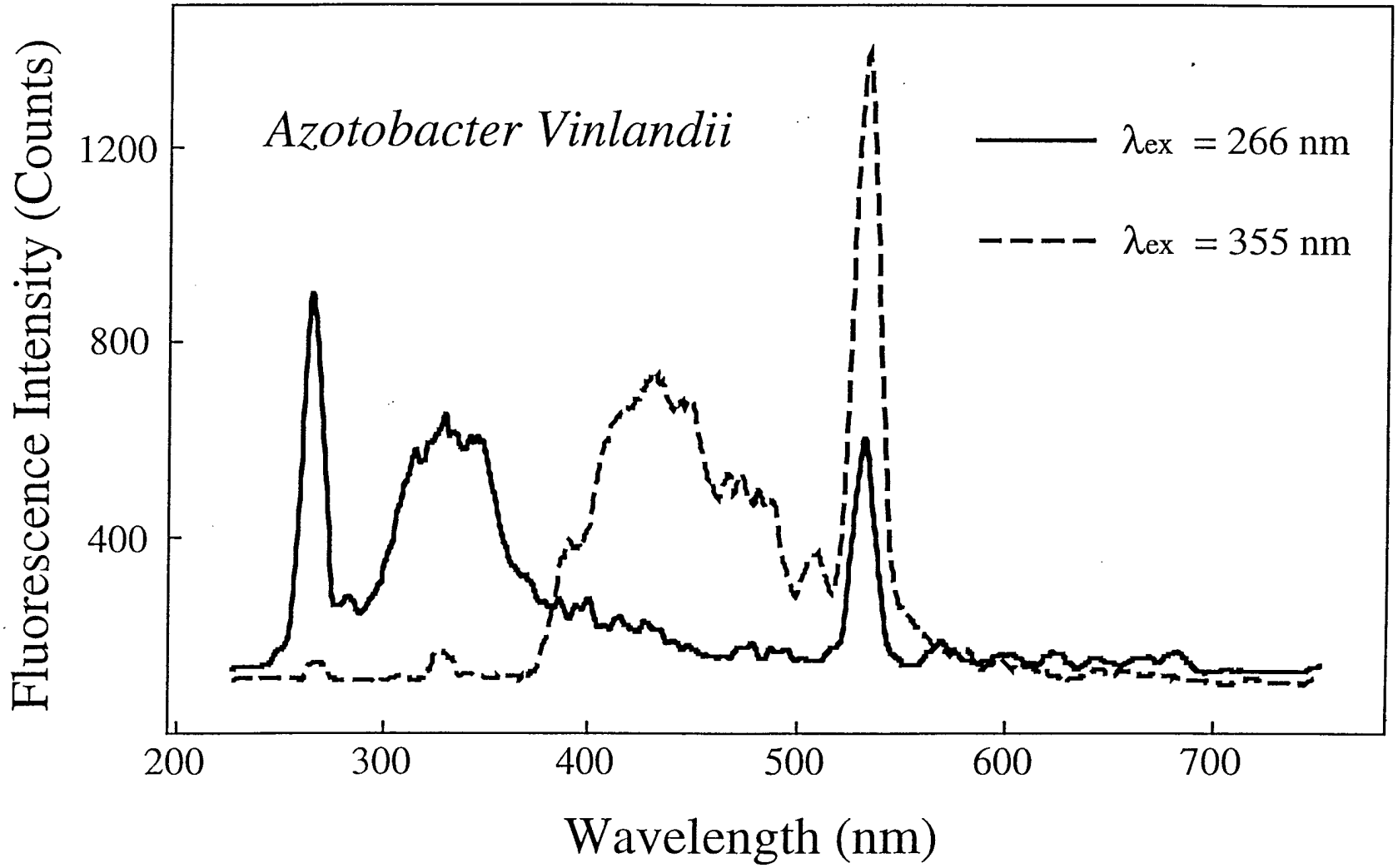

FIGURE 10. Same as Fig. 6, except for Azotobacter Vinlandii.